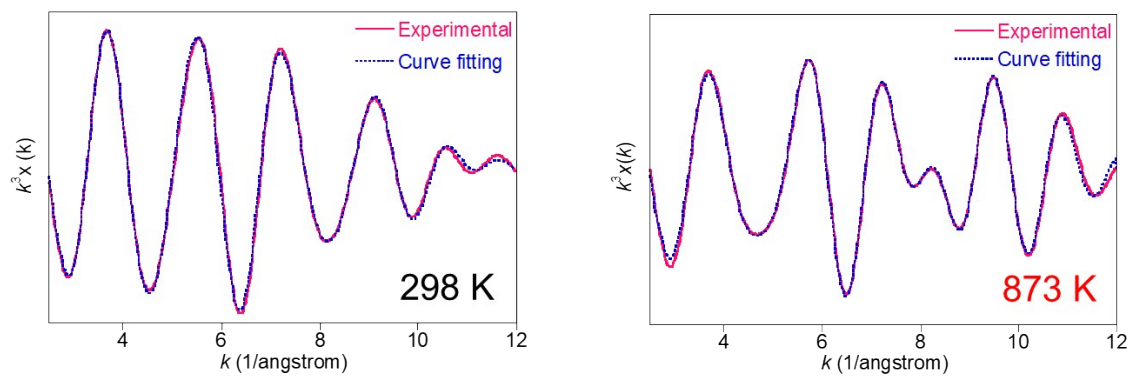


## **Supporting Information**

### **Room Temperature O Transfer from N<sub>2</sub>O to CO Mediated by Nearest Cd(I) Ions in MFI Zeolite Cavity**

## Supplementary figures and tables



**Fig. S1** Comparisons of the Fourier-transformed EXAFS ( $2 < k < 12 \text{ \AA}^{-1}$ ) with the curve fitting data: (left) 298 K- and (right) 873 K-evacuated samples.

**Table S1** Qualitative EXAFS analysis of Cd–O and Cd–Cd contributions.

Sample	1st (Cd–O)			2nd (Cd–Cd)		
	CN	$R$ [Å]	$\sigma^2$ [Å <sup>2</sup> ]	CN	$R$ [Å]	$\sigma^2$ [Å <sup>2</sup> ]
298 K-evacuated CdMFI	7.0	2.32	0.013	1.1	3.02	0.013
873 K-evacuated CdMFI	3.5	2.27	0.015	<b>0.9</b>	<b>2.67</b>	0.009

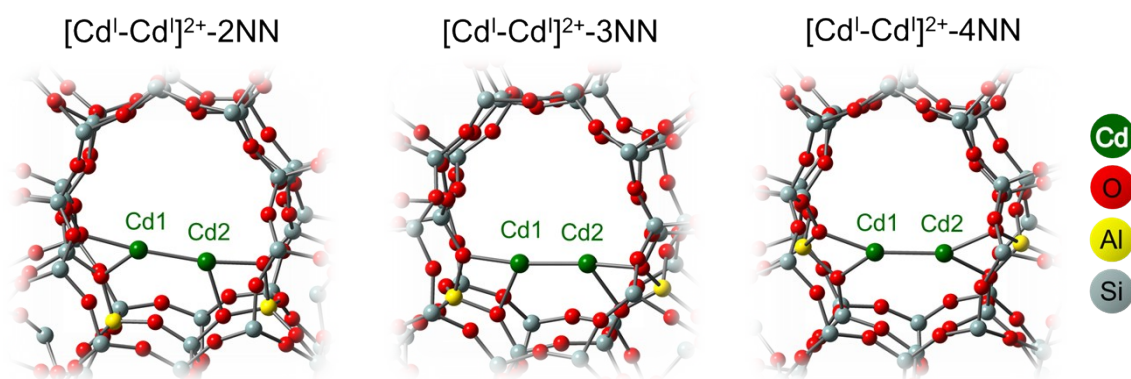


**Fig. S2** Optimized  $[\text{Cd}^{\text{I}}-\text{Cd}^{\text{II}}]^{2+}$ -MFI models, i.e.,  $[\text{Cd}_2]^{2+}-[\text{Al}_2\text{Si}_{90}\text{O}_{151}\text{H}_{66}]^{2-}$  clusters, having different Al arrays.

**Table S2** Selected DFT parameters of the  $[\text{Cd}^{\text{I}}-\text{Cd}^{\text{II}}]^{2+}$ -MFI models shown in Fig. S2: Cd–Cd distance ( $R_{\text{Cd1}-\text{Cd2}}$ ), natural charge ( $q_{\text{Cd1}}$ ,  $q_{\text{Cd2}}$ ), and  $\sigma-\sigma^*$  energy ( $E_{\sigma-\sigma^*}$ ).

Sites	$R_{\text{Cd1}-\text{Cd2}}$ [ $\text{\AA}$ ]	$q_{\text{Cd1}}^{\text{a}}$	$q_{\text{Cd2}}^{\text{a}}$	$E_{\sigma-\sigma^*}$ [ $\text{cm}^{-1}$ ]
$[\text{Cd}^{\text{I}}-\text{Cd}^{\text{II}}]^{2+}$ -2NN	2.63	+0.68	+0.75	38250
$[\text{Cd}^{\text{I}}-\text{Cd}^{\text{II}}]^{2+}$ -3NN	2.63	+0.71	+0.73	40430
$[\text{Cd}^{\text{I}}-\text{Cd}^{\text{II}}]^{2+}$ -4NN	2.69	+0.72	+0.74	40650

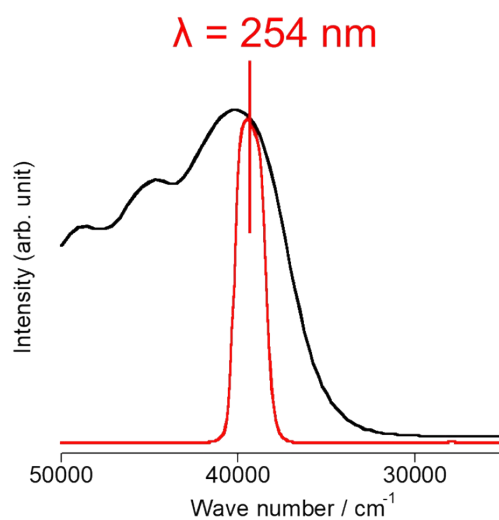


**Fig. S3** Energy distributions of the 254 nm light applying to the photoactivation of the Cd<sup>I</sup>-Cd<sup>I</sup> bond (red line). For comparison, the UV-vis spectrum of the 873 K-activated CdMFI sample is included (black line). The 254 nm light was generated using a 254 nm band pass filter.

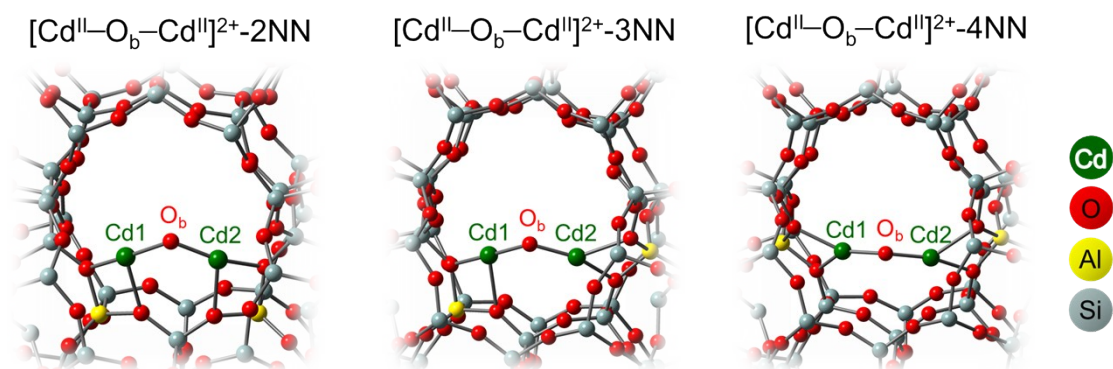


**Fig. S4** Optimized  $[\text{Cd}^{\text{II}}-\text{O}_b-\text{Cd}^{\text{II}}]^{2+}$ -MFI models, i.e.,  $[\text{Cd}_2\text{O}]^{2+}-[\text{Al}_2\text{Si}_{90}\text{O}_{151}\text{H}_{66}]^{2-}$ , having different Al arrays.

**Table S3** Selected DFT parameters of the  $[\text{Cd}^{\text{II}}-\text{O}_b-\text{Cd}^{\text{II}}]^{2+}$ -MFI models shown in Fig. S4: bond distance ( $R_{\text{Cd1}-\text{O}_b}$ ,  $R_{\text{Cd2}-\text{O}_b}$ ,  $R_{\text{Cd1}-\text{Cd2}}$ ), bond angle ( $\angle\text{Cd}-\text{O}_b-\text{Cd}$ ) natural charge ( $q_{\text{Cd1}}$ ,  $q_{\text{Cd2}}$ ,  $q_{\text{O}_b}$ ), and LMCT energy ( $E_{\text{LMCT}}$ ).

Sites	$R_{\text{Cd1}-\text{O}_b}$ [Å]	$R_{\text{Cd2}-\text{O}_b}$ [Å]	$R_{\text{Cd1}-\text{Cd2}}$ [Å]	$\angle\text{Cd}-\text{O}_b-\text{Cd}$ [°]	$q_{\text{Cd1}}$	$q_{\text{Cd2}}$	$q_{\text{O}_b}$	$E_{\text{LMCT}}^a$ [cm <sup>-1</sup> ]
2NN	2.01	2.02	3.39	114	1.26	1.26	-1.18	40900
3NN	2.01	2.01	3.49	121	1.27	1.30	-1.19	42000
4NN	2.00	2.01	3.60	128	1.31	1.32	-1.21	42400

<sup>a</sup>The most intense peak positions in the UV-vis spectra calculated by TD-DFT are described.

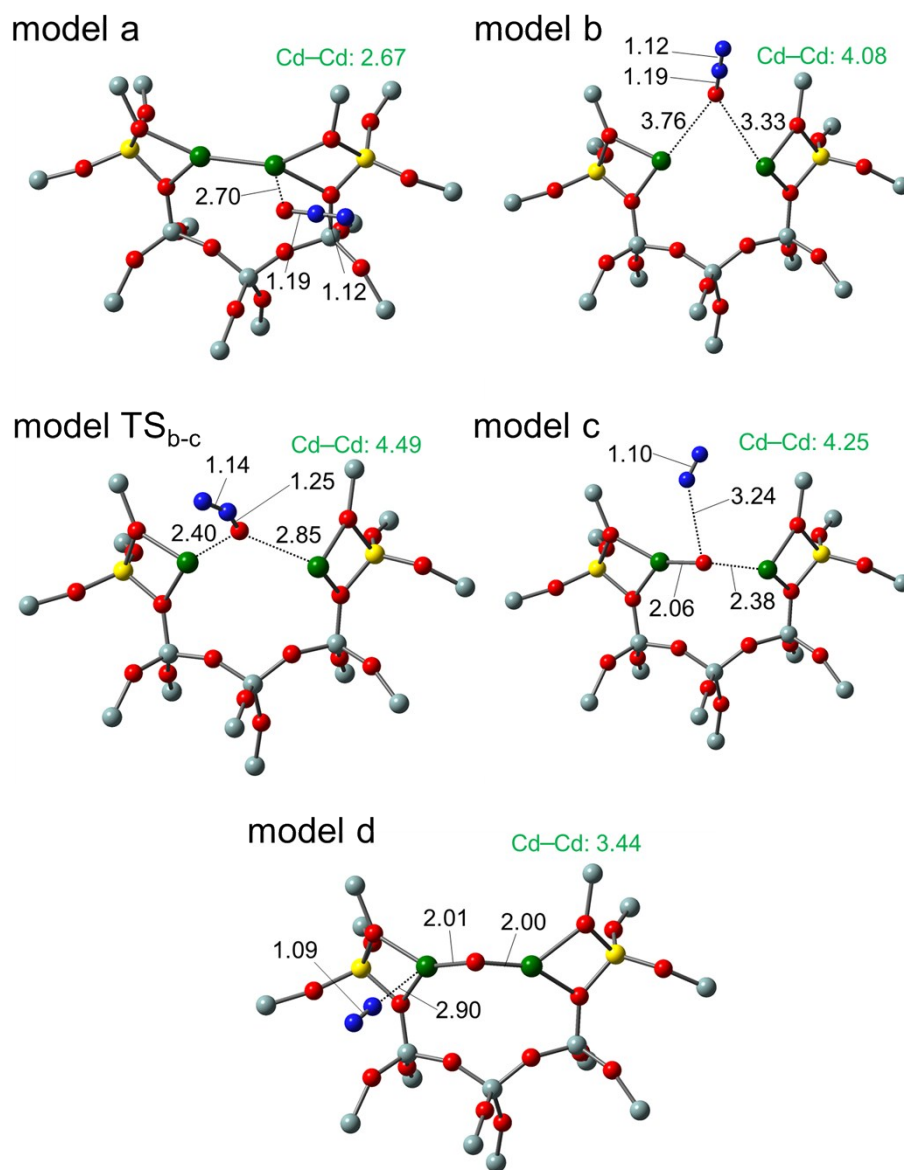


**Fig. S5** Structural details of the optimized geometries ( $[\text{Cd}_2\text{N}_2\text{O}]^{2+}$ - $[\text{Al}_2\text{Si}_{15}\text{O}_{16}\text{H}_{36}]^{2-}$ ,  $S = 0$  or  $1$ ) shown in Fig. 8, where terminated H atoms were omitted. Selected bond lengths are given as black and green numbers (Å).

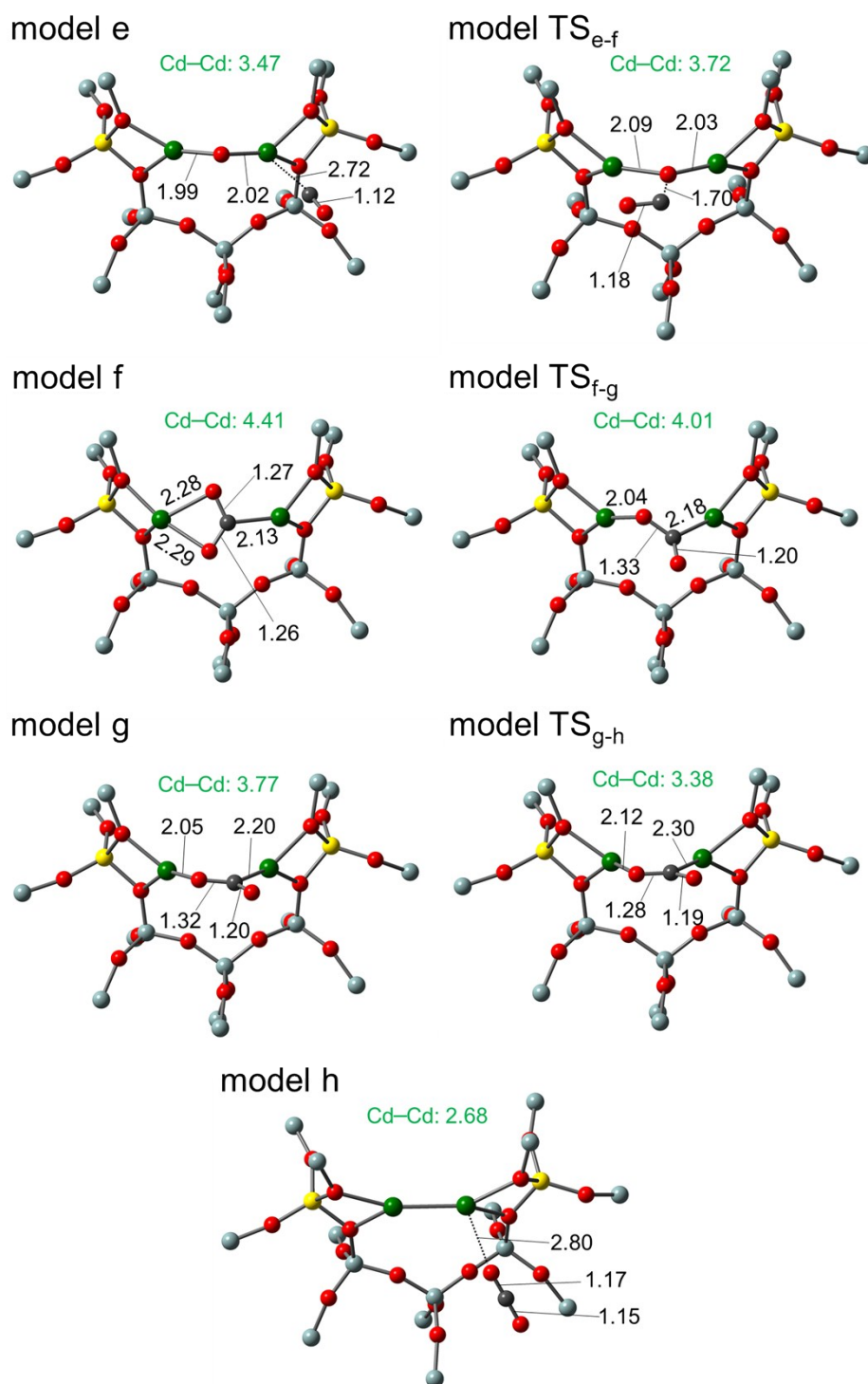


**Fig. S6** Structural details of the optimized geometries ( $[\text{Cd}_2\text{CO}_2]^{2+}$ - $[\text{Al}_2\text{Si}_{15}\text{O}_{16}\text{H}_{36}]^{2-}$ ,  $S = 0$ ) shown in Fig. 10, where terminated H atoms were omitted. Selected bond lengths are given as black and green numbers (Å).